Frequency-Domain Methods for Characterization of Pulsed Power Diagnostics*

A.D. White, R.A. Anderson, T.J. Ferriera, D.A. Goerz
Lawrence Livermore National Laboratory, PO Box 808, L-153
Livermore, CA 94550, USA

Abstract

This paper discusses methods of frequency-domain characterization of pulsed power sensors using vector network analyzer and spectrum analyzer techniques that offer significant simplification over time-domain methods, while mitigating or minimizing the effect of the difficulties present in time domain characterization. These methods are applicable to characterization of a wide variety of sensors.

I. INTRODUCTION

Pulsed power sensors such as B-dot probes and Rogowski Coils are frequently used in experimental pulsed power platforms with accuracies limited by the accuracy with which such sensors can be characterized. A straightforward method of characterizing such sensors is to compute the sensor response by comparing the probe output to a known system input. Using time-domain pulsed methods, accurate characterization of such sensors can be difficult, for several reasons.

In both capacitively and explosively driven pulsed power experiments, the frequency content of the signals to be measured is often low (kHz to hundreds of kHz). Attempting to characterize sensors using low frequency signals often results in insufficient SNR of the digitized sensor output—a B-dot probe with an *in-situ* sensitivity of a 10 pV per A/s subject to a 100 kHz 100 A input signal will produce an output of about 600 μV—only about 3.5 bits on a 0.25 Volt full-scale 12-bit digitizer.

When the reference signal used for comparison with the sensor output comes from a current viewing resistor (CVR) or current transformer (CT), the sensor output must be integrated for comparison with the reference. Rigor must be applied to prevent introduction of error here, either from droop or loss in the hardware integrator or bias from infinite DC gain of software integration.

Lastly, any frequency dependence in the response of the sensor is difficult to observe from the digitizer time records alone. If frequency dependence does exist, it must be removed from the digitizer records by applying Fourier Transforms and deconvolution to the measured data, which is an undesirable inconvenience.

An alternate method to time-domain pulsed methods is to use a vector network analyzer, or swept-frequency source and spectrum analyzer. Such methods minimize several of the above issues. The dynamic range of modern network analyzers is greater than 130 dB; accurate sensing of signals with amplitudes in the μV is possible. The need to perform integration is avoided by instead using a least-squares-fit to frequency domain-data to determine the frequency response. Any frequency dependence in the frequency response can either be observed directly from the measured data, or determined with a few linear least-squares fits to the data.

II. IDEAL SENSOR RESPONSE

The form of the frequency response of a time-derivative probe can be determined from inspection of the Fourier transform pair

$$\frac{df(t)}{dt} \leftrightarrow j\omega F(j\omega). \qquad (1)$$

The output of a derivative sensor is dependent on the area of the loops and the orientation relative to the incident field. Embodying these factors in a sensitivity ±*S* with units V/A/s, Eq. (1) can be modified to yield:

$$\pm S\frac{dx(t)}{dt} \leftrightarrow \pm Sj\omega X(j\omega) = H(j\omega)X(j\omega) = Y(j\omega). \qquad (2)$$

Eq. (2) states that in the frequency domain, the probe output *Y(jω)* with units V is equal to the frequency response *H(jω)* with units V/A multiplied by the input signal *X(jω)* with units A. The magnitude of the frequency response *H(jω)* is of the form of a line with slope *S.* The argument of the frequency response *H(jω)* is positive or negative π/2, the sign dependent probe orientation, which manifests itself in whether a positive or negative derivative of the input was taken.

* This work performed under the auspices of the U.S. Department of Energy by Lawrence Livermore National Laboratory under Contract DE-AC52-07NA27344.

Report Documentation Page

Form Approved
OMB No. 0704-0188

Public reporting burden for the collection of information is estimated to average 1 hour per response, including the time for reviewing instructions, searching existing data sources, gathering and maintaining the data needed, and completing and reviewing the collection of information. Send comments regarding this burden estimate or any other aspect of this collection of information, including suggestions for reducing this burden, to Washington Headquarters Services, Directorate for Information Operations and Reports, 1215 Jefferson Davis Highway, Suite 1204, Arlington VA 22202-4302. Respondents should be aware that notwithstanding any other provision of law, no person shall be subject to a penalty for failing to comply with a collection of information if it does not display a currently valid OMB control number.

1. REPORT DATE	2. REPORT TYPE	3. DATES COVERED
JUN 2009	**N/A**	**-**

4. TITLE AND SUBTITLE	5a. CONTRACT NUMBER
Frequency-Domain Methods for Characterization of Pulsed Power Diagnostics	5b. GRANT NUMBER
	5c. PROGRAM ELEMENT NUMBER
6. AUTHOR(S)	5d. PROJECT NUMBER
	5e. TASK NUMBER
	5f. WORK UNIT NUMBER
7. PERFORMING ORGANIZATION NAME(S) AND ADDRESS(ES) **Lawrence Livermore National Laboratory, PO Box 808, L-153 Livermore, CA 94550, USA**	8. PERFORMING ORGANIZATION REPORT NUMBER
9. SPONSORING/MONITORING AGENCY NAME(S) AND ADDRESS(ES)	10. SPONSOR/MONITOR'S ACRONYM(S)
	11. SPONSOR/MONITOR'S REPORT NUMBER(S)

12. DISTRIBUTION/AVAILABILITY STATEMENT
Approved for public release, distribution unlimited

13. SUPPLEMENTARY NOTES
See also ADM002371. 2013 IEEE Pulsed Power Conference, Digest of Technical Papers 1976-2013, and Abstracts of the 2013 IEEE International Conference on Plasma Science. IEEE International Pulsed Power Conference (19th). Held in San Francisco, CA on 16-21 June 2013., The original document contains color images.

14. ABSTRACT
This paper discusses methods of frequency-domain characterization of pulsed power sensors using vector network analyzer and spectrum analyzer techniques that offer significant simplification over time-domain methods, while mitigating or minimizing the effect of the difficulties present in time domain characterization. These methods are applicable to characterization of a wide variety of sensors.

15. SUBJECT TERMS

16. SECURITY CLASSIFICATION OF:			17. LIMITATION OF ABSTRACT	18. NUMBER OF PAGES	19a. NAME OF RESPONSIBLE PERSON
a. REPORT	b. ABSTRACT	c. THIS PAGE			
unclassified	**unclassified**	**unclassified**	**SAR**	**4**	

III. MEASURING THE FREQUENCY RESPONSE

Fig. 1 shows the hardware and instrumentation setup to measure the frequency response of a B-dot probe in a coaxial 6'' airline test fixture.

A. Instrumentation

We use an Agilent 4395A Vector Network/Spectrum/Impedance analyzer. The bandwidth of this instrument is from 10 Hz to 500 MHz, with a dynamic range of 115 dB using an IF BW of 10 Hz. The RF source power of the network analyzer is limited to +15 dBm, or roughly 25 mA RMS into 50 Ω or 50 mA RMS into a short. We have found this to be the primary limitation of the instrument.

In measurements where the limited source power of the network analyzer is not of concern, an S-parameter test set or transmission/reflection test set can be used to provide a reference signal for comparison with the probe output. The transmission/reflection test set is simply a directional coupler and therefore requires that the test fixture (coaxial airline in Fig. 1, e.g.) be terminated with a 50 Ω load, while the S-parameter test set can be used with arbitrary terminating impedances, but typically only above tens or hundreds of kHz. The necessary measurement corrections are simplified when one of these can be used. Since our *in-situ* calibration hardware is typically not terminated in 50 Ω terminations, and since our bandwidths of interest are in the kHz and tens of kHz, we usually cannot use either of these test. Further, since our sensors are often fairly insensitive (on the order of 10^{-12} V/A/s), we often use external amplification of the network analyzer drive signal, which makes use of the aforementioned test sets problematic.

To achieve such external amplification of the source signal levels we use an Amplifier Research 350AH1 350 Watt 10 Hz – 1 MHz RF amplifier. This amplifier is capable of driving approximately 15 A RMS into our shorted coaxial airline test fixture, which greatly increases the dynamic range of our low-frequency measurements.

To measure the source signal and provide a reference signal to compare the probe output with, we use a calibrated Current Transformer (CT) between the amplifier output (or network analyzer output if no amplifier is used) and the test fixture input. This technique is only applicable at wavelengths much larger than the physical dimension of the test fixture and cabling. EMI must be considered when selecting a CT fixture. We prefer using a CT fixture that completely encloses the CT, and couples the CT output through a wipe-off feedthrough (see Fig. 2). This reduces coupling of current from the outside to the inside of the CT cables.

B. Coaxial Airline Test Fixture

The test fixture shown in Fig. 1 is a 6'' coaxial airline. The S-parameters of the airline have been measured and

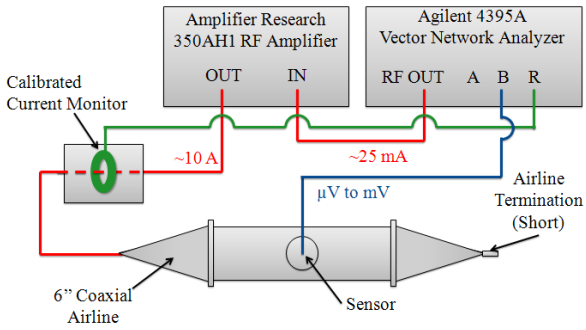

Figure 1. Instrumentation for performing B-dot frequency response measurement in a 6'' coaxial airline

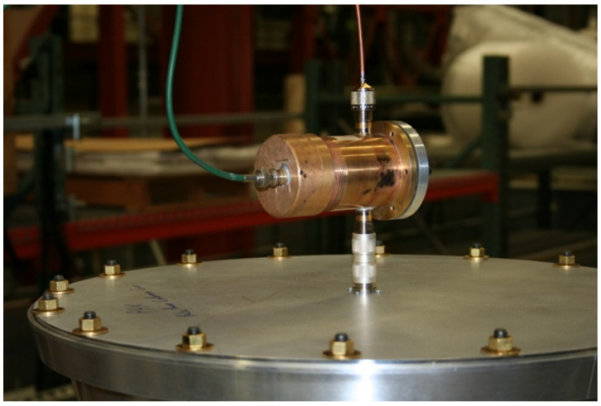

Figure 2. Enclosed CT fixture attached to experiment hardware. Type-N connectors are welded to the enclosure. The CT output is coupled through a BNC wipe-off feedthrough in the foreground.

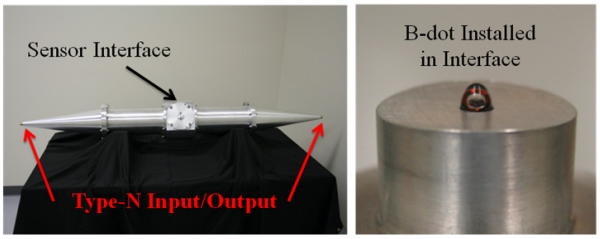

Figure 3. Coaxial airline (left) and B-dot (right). The B-dot shown consists of four loops of 0.005'' wire with an ID of 0.072''.

are shown in Figure 4. For frequencies less than 3.5 GHz, S_{11} is less than -18 dB and S_{21} is less than -0.2 dB. The airline and airline sensor interface for B-dot probes is shown in Figure 3. Different interfaces can be fabricated to allow installation and measurement of diagnostics with different geometries.

The coaxial airline is used to perform a functional check of our diagnostics prior to installation of the sensors into experiment hardware. This allows us to group sensors by sensitivity so that probes selected for experiments will have similar sensitivities. Since the airline represents a nearly ideal geometry, the probe response can be approximated fairly well from first principles. Deviation from the idealized response is

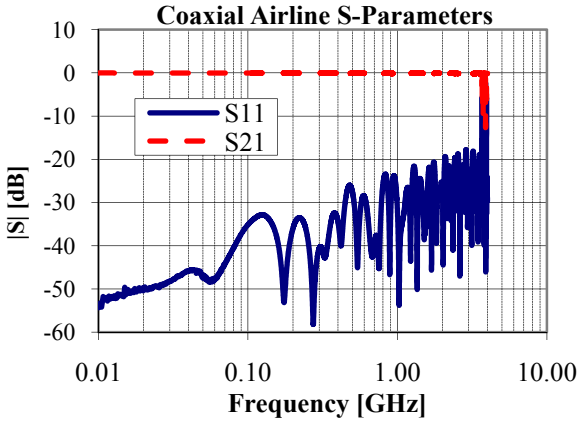

Figure 4. Measured S-parameters of coaxial airline shown in Fig. 3.

caused by the hole through which the B-dot is inserted (see Fig. 3). Surface current distribution near the hole affects flux distribution in the loops, and causes a decrease in probe sensitivity or effective area. This effect has slight frequency dependence, but results in roughly a 10%-20% decrease in effective area for a probe inserted as shown in Fig. 3. Inserting the loops further into the airline reduces the magnitude of this effect.

After calibration of sensors in the airline, we recalibrate the probes *in-situ* in the experimental hardware whenever possible (i.e., installed in a flux compression generator).

C. Measurement Procedure

With the instrumentation setup shown in Fig. 1, measurement of the frequency response is performed as described below.

The network analyzer is programmed to output a frequency sweep across the bandwidth of interest. The gain of the RF amplifier is adjusted to provide a drive current at the desired level.

The network analyzer is set to perform a measurement of the ratio of the signal on port B to the signal on port R. The quantities being measured at i points defined by the frequency sweep are:

$$\left(\frac{B}{R}\right)_i = \frac{V_{p,i}}{CT_i\, I_i}\left(\frac{G_B}{G_R}\right)_i = H(j\omega)_i \frac{1}{CT_i}\left(\frac{G_B}{G_R}\right)_i \qquad (3)$$

or

$$H(j\omega)_i = \left(\frac{B}{R}\right)_i CT_i \left(\left(\frac{G_B}{G_R}\right)_i\right)^{-1}, \qquad (4)$$

where, G_B and G_R are the unitless gains on network analyzer ports B and R, CT is the measured CT sensitivity with units V/A, V_p is the voltage at the sensor output, and I is the current flowing in the test fixture.

The quantities G_B and G_R in Eqs. (3) and (4) represent gains on the network analyzer ports that are near but not precisely unity. Agilent specifies the absolute accuracies of uncorrected B/R measurements as ±2 dB. To remove errors produced by these inaccuracies, the ratio of the port gains can be measured and applied as a correction to measured sensor data, as shown in Eq. (4). This is accomplished by connecting the RF output of the network analyzer directly to port B and measuring port B alone, then connecting the RF output to port R and measuring port R alone, then taking the ratio at each frequency point i of the two files. Note that if the port impedances are different, this approach will contain error, but in our experience the port impedances have been nearly identical.

If a transmission/reflection test set is used on the network analyzer, computation of the frequency response is simplified since the CT is no longer necessary, and since internal network analyzer calibration can be used to compensate for port gain errors. In this case, the terms containing port gains in Eqs. (3) and (4) can be eliminated, and the CT sensitivity in V/A replaced with 50 V/A, the impedance of port R. Similar simplifications are possible when an S-parameter test is used

Since Eqs. (3) and (4) make no assumptions about the form of the frequency response $H(j\omega)$, they are valid for not just time-derivative sensors, but sensors with any frequency response described with units V/A. If a voltage probe or directional coupler is used to provide the reference signal instead of a CT, frequency responses with units of V/V can be measured.

Correction for cable loss, attenuator loss, or other instrumentation can be measured and applied to frequency response measurements in a manner identical to the network analyzer port gain correction. In most of our characterizations, we have no attenuators, and use short low-loss cables, making such corrections unnecessary.

D. Interpreting the B-dot Frequency Response

When the probe response is near that of an ideal B-dot, the frequency response will take the form from Eq. (2):

$$H(j\omega)_i \approx \pm Sj\omega_i = \pm Sj2\pi f_i. \qquad (5)$$

The measured frequency response is of the form of a line with slope $2\pi S$ and argument $\pm j$.

To compute a scalar probe sensitivity S from the measured frequency response, we compute the value of S that minimizes $\boldsymbol{\varepsilon}$:

$$\varepsilon = \left\| S\, f_i - \frac{|H(j\omega)_i|}{2\pi} \right\|, \qquad (6)$$

which is simply the least-squares linear fit to the magnitude of the frequency response divided of 2π. Implicit in Eq. (6) is the assumption that the fit has a y-

intercept of 0 at f = 0 Hz, which is well understood for a B-dot probe.

The polarity of the B-dot probe can be determined from the argument of the frequency response, since:

$$arg(H(j\omega)_i) \approx arg(\pm Sj2\pi f_i) = \pm\frac{\pi}{2}. \qquad (7)$$

Recall from Eq. (2) that a probe taking the positive time derivative will have an argument of $+\pi/2$, and a probe taking a negative time derivative will have an argument of $-\pi/2$.

E. Measured Data

Measured data from both a positive and negative polarity B-dot probe are shown in Fig. 5.

The B-dot probes were formed by wrapping insulated copper wire with 0.005 in. radius around a 0.072 in. mandrel to form ten loops. The leads of the loops were twisted into a twisted pair, and the loops and leads were inserted into a quartz tube with an OD of 4 mm. The interior of the tube was potted with epoxy. An SSMA connector was epoxied to the quartz tube then soldered to the twisted pair. The orientation of the probe is fixed by a pin that is located on a flange that is epoxied to the quartz tube. When the probe is installed in either calibration or experimental hardware, the pin is inserted into a corresponding socket that fixes the probe orientation and prevents rotation of the probe.

The data shown in Fig. 5 has been corrected for network analyzer port gains and CT response, as described by Eq. (4). It has also been scaled by $1/2\pi$, as described in Eqs. (5) and (6), so that the slope of the data is the sensitivity in V/(A-Hz) or V/A/s. Thus what is shown in Fig. 5a) and b) are the magnitudes of the frequency response $|H(j\omega)|$, and in 5c) the argument of the frequency response $arg(H(j\omega))$.

The linear least-squares fit to the data shown in Fig. 5 was produced by applying Eq. (6) to the frequency response. The parameters produced by the fit for the positive probe in Fig. 5a) are: S = 94.44E-12 V/(A-Hz) = +94.45 V/MA/μs, $R^2 = 0.99997$. The parameters produced by the fit for the negative probe in Fig. 5b) are S = -94.46E-12 V/(A-Hz) = 94.46 V/MA/μs, $R^2 = 0.99997$. The signs on the sensitivities were determined by inspecting the phase of the probe responses, as described by Eq. (7), and shown in Fig. 5c). These sensitivities (magnitudes and signs) fully characterize the B-dot probes across the bandwidth of the measurement.

IV. SUMMARY

A method of using frequency domain measurement techniques to characterize pulsed power diagnostics is discussed. The principle advantages of frequency domain characterization are simplicity, large dynamic range, and the ability to directly observe the frequency response of a sensor. These methods are applicable across large bandwidths (hundreds of Hz to GHz) to a wide variety of devices (B-dot and D-dot probes, E probes, current monitors, Rogowski coils, etc.).

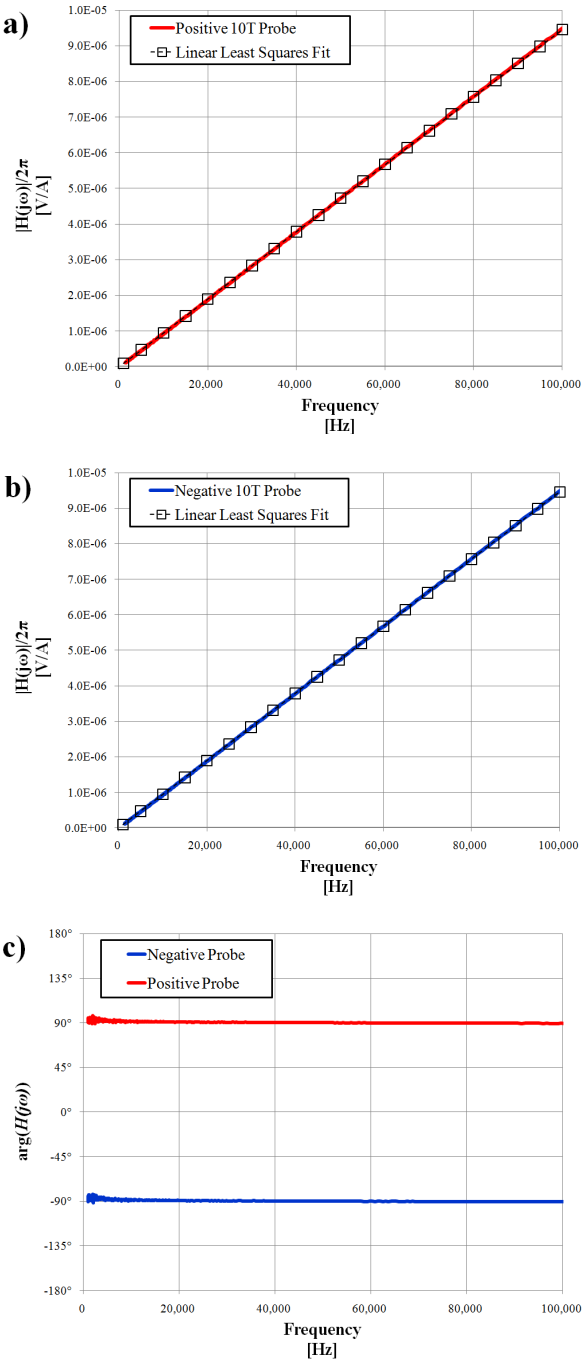

Figure 5. The magnitudes of the frequency responses $|H(j\omega)|$ for a positive and negative ten loop probe are shown in a) and b), the argument of the frequency response $arg(H(j\omega))$ for the same probes are shown in c).